

## FORMAMIDE AS A ROBUST ALTERNATIVE TO WATER FOR PLASTICIZING POLYELECTROLYTE COMPLEXES

*Sarriah Hassoun, Zachary A. Digby, Nagham Abou Hamad, Joseph B. Schlenoff\**

Department of Chemistry & Biochemistry

The Florida State University, Tallahassee, FL 32306, USA

Keywords: coacervate, doping, salt resistance, ion transport, rheology

\*Email: [jschlenoff@fsu.edu](mailto:jschlenoff@fsu.edu)

## Abstract

Polyelectrolyte complexes, PECs, are glassy and brittle when dry but may be plasticized with water. Though hydrated PECs contain a high proportion of water, many still exhibit a glass transition in the 0 to 100 °C range. The apparently unique effectiveness of water as a plasticizer of PECs has been an obstacle to further developments in applications and in fundamental studies of PEC properties. In this work it is shown that formamide is an excellent and even superior solvent for plasticizing PECs, substantially decreasing glass transition temperatures relative to those of hydrated PECs when formamide is used as a solvent instead. The affinities of PECs for water and formamide, indicated by the (exothermic) enthalpies of solvent swelling of dry PECs, are comparable. Ion transport dynamics revealed similar lifetimes, about 1 ns, of charge pairs within a PEC solvated with water compared to formamide, despite the differences in their dielectric constants. Ion transport dynamics, which depend on the mobility of pendant groups, have lower cooperativity than those of the polymer backbone. The use of formamide is a significant experimental variable for reducing the glass transition temperature/viscosity of complexed polyelectrolytes and can turn a solidlike hydrated complex into a fluidlike coacervate.

## Introduction

Plasticizers are small molecules widely used to soften brittle or glassy polymers.<sup>1</sup> For example, polyvinyl chloride, used in rigid pipes, becomes soft and flexible with the addition of organic plasticizers.<sup>2</sup> For hydrophilic materials, water can be an extremely effective plasticizer. In the biopolymers realm; aggrecan, with a charged bottle-brush polyelectrolyte architecture, maintains a high osmotic pressure in cartilage, which endows this biomaterial with elastic and shock-absorbing properties.<sup>3</sup> Proton conducting membranes, such as Nafion, used in fuel cells, require proper hydration in order to transport ions.<sup>4</sup>

Polyelectrolyte complexes, PECs, are blends of oppositely-charged polymers.<sup>5–8</sup> Formed by spontaneous phase separation from mixed solutions of polyelectrolytes due to the pairing of opposite charges, PECs retain a high weight percent of water when in contact with aqueous solutions. This water is essential to all the physical properties of PECs, including mechanical properties and ionic conductivity.<sup>9</sup> Michaels, who explored the processing and properties of PECs,<sup>5–6</sup> described the strong plasticizing effects of water, which transforms dry PECs from stiff and brittle to soft and flexible. Hydrated PECs that are above their glass transition temperature,  $T_g$ , have liquidlike properties and are generally termed “coacervates,” following Bungenberg de Jong’s early work on liquid-liquid phase separations of biopolymers.<sup>7</sup> Complexation/coacervation may be driven by mechanisms other than pairing between charges.<sup>8</sup>

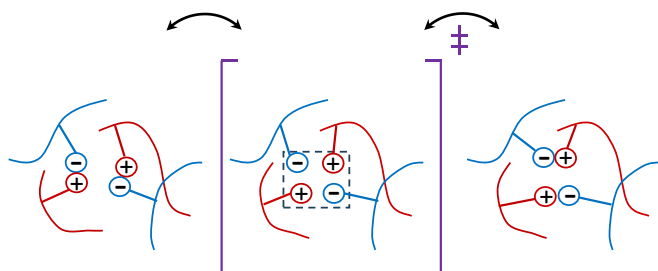
Though the plasticizing effect of water on PECs was generally known in early work, quantitative explorations of this phenomenon were rare, perhaps because the dried material is so brittle.<sup>5–6</sup> The more recent ultrathin “multilayer” format of PECs<sup>10</sup> allowed the modulus of dried films to be measured using scanning probe microscopy or nanoindentation<sup>11–13</sup> and buckling methods.<sup>14–15</sup> Some PECs were found to have elastic modulii in the several GPa range.<sup>11, 14, 16</sup> Extrusion of hydrated PECs in the absence of added salt aligns the chains and leads to increased modulus and toughness.<sup>17</sup> For example, a fiber extruded in this way from a PEC of poly(diallyldimethylammonium), PDADMA, and poly(styrene sulfonate), PSS, had a modulus of 1.5 GPa and toughness of 9.1 MJ m<sup>–3</sup> when dry and could even be tied in knots.<sup>17</sup>

As with neutral, hydrophilic polymers,<sup>18</sup> the modulus of PECs depends strongly on relative humidity<sup>15, 19–20</sup> which controls their water content.<sup>21–22</sup> Hariri et al.<sup>12</sup> used the osmotic stressing agent poly(ethylene glycol) to regulate the water content in bulk and thin film PECs made from PDADMA and PSS. The initial water extracted from the PEC had little influence on the modulus

until the water content reached about 40 wt%, whereupon the PEC became stiffer.<sup>12</sup> Ohno et al.<sup>23</sup> employed differential scanning calorimetry, DSC, to identify strongly versus weakly bound water in PECs. More recently, Lutkenhaus and coworkers correlated  $T_g$  in PECs to the amount of water<sup>24</sup> and were able to differentiate between water in various states using DSC and computational methods.<sup>25</sup> In addition to their effective plasticization by water, PECs can also be softened by breaking the charge pairing between positive,  $\text{Pol}^+$ , and negative,  $\text{Pol}^-$ , polyelectrolyte repeat units.<sup>26</sup> This “saloplasticity” is reversible and allows glassy PECs to be processed into many bulk formats.<sup>27</sup>

The selection of small molecules other than water available for plasticizing PECs is surprisingly small.<sup>28</sup> Many polar solvents cannot swell PECs, possibly limited by the mesh size of their dense ionic crosslinking.<sup>28</sup> Ionic liquids, with chemical and charge compositions similar to those of PECs, are also unable plasticize or dope PECs by themselves without water.<sup>29</sup> A deep eutectic solvent required the addition of a cosolvent such as ethylene glycol or water in order to dissolve a PEC.<sup>30</sup> Michaels addressed the challenge of swelling and dissolving PECs by using ternary mixtures of water, acetone and a salt.<sup>31</sup>

It is not clear whether the mechanism of plasticizer action in charged polymers differs from that in neutral polymers. Although both benefit from the free volume added by small molecules, as well as the dilution of contacts and entanglements, the mobility of PEC chains in the fluid state, far above  $T_g$ , depends on the dynamics of  $\text{Pol}^+\text{Pol}^-$  pair making and breaking.<sup>26</sup> In particular, flow properties of undoped (salt ion free) liquid-like PECs are thought to be derived from the rapid exchange of neighboring  $\text{Pol}^+\text{Pol}^-$  pairs of polyelectrolyte repeat units.<sup>26</sup> It could be argued that a high dielectric medium should stabilize the separation of charges in the possible pair exchange transition state, shown in Scheme 1.



**Scheme 1.** Rearrangement of  $\text{Pol}^+\text{Pol}^-$  pairs may involve a charge-separated transition state.

Using a solvent with a higher dielectric constant than water may result in PECs with weaker interactions. The dielectric constant of water and formamide<sup>32</sup> are 78 and 110, respectively at 25 °C. Individual polyelectrolytes can be dissolved in formamide. Formamide and water have many similar properties, such as self-association, hydrogen bonding, a large dipole moment, and fast reorientational jump dynamics.<sup>33</sup> The two solvents show almost ideal mixing,<sup>34</sup> but the temperature range of liquid formamide (2 – 210 °C) is much wider than that of water. Formamide is often used in structural biology studies. Similar to water, formamide is capable of four hydrogen bonds, is a strong H-bond donor, and a stronger H-bond acceptor than water.<sup>35</sup> Formamide is known to destabilize DNA duplexes.<sup>36</sup> This destabilization occurs with cooperative  $\pi$ -electron charge transfer interactions, forming bidentate pairs with DNA bases.<sup>37-38</sup> Formamide thereby lowers the melting temperatures of DNA by 0.65 °C per percent volume fraction.<sup>39</sup> Kamineni et al. demonstrated the ability to make polyelectrolyte multilayers of PAH and PSS dissolved in formamide,<sup>40</sup> but this solvent has not been used in bulk PECs.

The purpose of this work is to introduce formamide as an alternative to water for fundamental studies and applications of PECs. Both thermodynamic and kinetic aspects of the influence of formamide on PEC properties are explored.

## Experimental

### Materials

Poly(diallyldimethylammonium chloride) (PDADMAC, molar mass 200,000 – 350,000 g mol<sup>-1</sup>) and poly(4-styrenesulfonic acid, sodium salt) (PSSNa, molar mass 75,000 g mol<sup>-1</sup>) were obtained from Sigma-Aldrich and purified by dialysis. Poly(vinylbenzyl trimethylammonium chloride) (PVBTAC, 27 wt% in water, 100,000 g mol<sup>-1</sup>) was from Scientific Polymer Products and used without further purification. Sodium bromide was supplied by Sigma-Aldrich and dried at 110 °C for 24 h. Formamide (ReagentPlus®, >99.0%) from Sigma-Aldrich was used as received. All solutions were prepared using deionized water (18 MΩ cm Barnstead, Nanopure).

### Methods

**Critical Salt Concentration, CSC.** UV-visible spectroscopy (UV-vis) was performed using a Cary 100 Bio UV-vis spectrometer to determine the CSC of PECs in formamide solutions of NaBr. Two methods of determining the CSC were employed: the forward and reverse methods. In both, scattering (turbidity) of a 10 mg mL<sup>-1</sup> PEC solution was monitored at 390 nm. In the forward method, where aliquots of concentrated NaBr in formamide were added to a suspension of PEC particles in formamide, the CSC was taken to be the point where the turbidity dropped to nearly zero absorbance. The reverse method consisted of adding known amounts of formamide to PEC dissolved in NaBr just past the CSC and identifying the [NaBr] at which the turbidity started to increase.

**Isothermal Titration Calorimetry.** Isothermal calorimetry (ITC) was performed using a VP-ITC (MicroCal Inc.) calorimeter using water or formamide as solvents. Prior to the aqueous experiments, the ITC was calibrated with an internal y-axis calibration followed by a standard titration between hydrochloric acid and Tris base. All samples were degassed for 10 min at room temperature. Approximately 300 μL of 10 mM polycation (concentrations are based on the polymer repeat unit) in 0.01 M NaBr was loaded into the syringe. Ten microliters of the syringe solution were manually discharged from the syringe to relieve any back pressure from the loading process. Prior to filling, the sample cell (1.4138 mL) was washed with 0.5 mM polyanion in 0.01 M NaBr. The syringe was rotated at 260 rpm in the sample cell with an injection size of 4 μL per aliquot at a rate of 0.50 μL s<sup>-1</sup>, with 240 s between injections. The heat flow was recorded as a function of time at 25.0 °C for all samples. Enthalpies were calculated by summing the total heat generated to the 1:1 Pol<sup>+</sup>:Pol<sup>-</sup> end point with a correction for the background dilution enthalpy. To perform the ITC experiments in formamide, the reference cell was rinsed then filled with formamide. The reference cell was sealed and the sample cell was similarly rinsed and filled. A titration of formamide into formamide was performed to ensure that there was no leftover water or polyelectrolyte in the system. Formamide (with 0.01 M NaBr) experiments were carried out in conditions identical to those of the aqueous experiments.

**Solvent Swelling Calorimetry.** The enthalpies of solvent swelling of dry PECs were determined using a Parr 6755 solution calorimeter charged with 100.0 mL formamide. The dry PECs were finely ground, passed through a 100 μm sieve, dried again at 120 °C, sealed while hot, and stored in an argon filled dry box. Samples were weighed into a PTFE sample dish in the glovebox. The sample dish was sealed and transferred to the calorimeter. After a short temperature equilibration period the sample was plunged into the formamide and the temperature increase, ΔT, was measured with a Parr 6772 calorimetric thermometer. A linear temperature ramp was subtracted from the data to account for temperature drift. The calorimeter was calibrated as described previously<sup>37</sup> to provide a calorimeter constant C of 539.2 J K<sup>-1</sup> when charged with 100.0 mL water. C for 100.0 mL formamide was determined by subtracting the contribution of the water (= 539.2 – (4.18 × 100) = 121.2 J K<sup>-1</sup>) and adding the heat capacity of 100 mL (= 113 g) of formamide of specific heat capacity 2.39 J g<sup>-1</sup> K<sup>-1</sup> to obtain a constant of 391.4

$\text{J K}^{-1}$  for the formamide experiments. The enthalpy of swelling,  $\Delta H_{\text{swell}}$  ( $\text{J g}^{-1}$ ), was calculated from  $\Delta H = C\Delta T/m_{\text{sample}}$ , where  $m_{\text{sample}}$  is the mass of the sample (g).

**PEC Tablet Preparation.** The starting PECs of PDADMA/PSS and PVBTA/PSS used here have been described and were determined to be stoichiometric in previous works.<sup>41–42</sup> The dried PECs were ground into a fine powder and placed into an 8 mm diameter stainless steel mold with a drop of formamide. A weight of approximately 8 kg was placed onto the mold, and the PEC was pressed into a circular tablet over 24 h under pressure. These tablets were used for ATR-FTIR, salt doping, and rheology.

**ATR-FTIR Spectroscopy.** Attenuated total internal reflection–Fourier transform infrared (ATR-FTIR) spectra were collected using a ThermoScientific Nicolet iS20 spectrometer with a Pike MIRacle universal ATR attachment fitted with a single-reflection diamond/ZnSe crystal and a high-pressure clamp. A stainless-steel well was machined to fit onto the crystal plate to allow solid samples to be pressed onto the crystal while remaining immersed in solution. The number of scans coadded was 32 and resolution was  $4 \text{ cm}^{-1}$ .

**Rheology.** Measurements of the linear viscoelastic response (LVR) were performed using a strain-controlled rheometer (DHR-3, TA Instruments) with Peltier temperature control. An 8 mm parallel plate geometry was used throughout. A custom-designed lower plate had a reservoir for solutions with a cap to prevent evaporation. Prior to loading, all PECs were soaked in 0.01 M NaBr solutions with varying water and formamide contents for 24 h, which were also added to the solution reservoir to maintain the PECs in a fully solvated state. The PECs were first transferred onto the upper plate. The upper plate was then lowered onto the lower plate. An axial force of 0.5 N was applied for PECs containing 0.25 - 1.00 mole fraction (25% - 100%) formamide. A strain of 0.5% was used and verified to be in the linear viscoelastic response region. PECs soaked in solutions containing less than 25% formamide had an axial force of 1.0 N (and a strain of 0.02%). The modulus as a function of temperature from 5 to 95 °C was determined at 0.1 Hz with a ramp rate of  $2 \text{ }^{\circ}\text{C min}^{-1}$  (0.05 and 0 mole fraction formamide had a ramp rate of  $1 \text{ }^{\circ}\text{C min}^{-1}$ ).

**Salt Doping.** Radiolabeling experiments were performed to determine the doping level, or the salt content, of PDADMA/PSS PEC tablets exposed to solutions of various [NaBr] in formamide. A  $^{22}\text{Na}$ -labeled solution was prepared as follows: to 4 mL of 0.1 M NaBr in formamide was added 1  $\mu\text{Ci}$   $^{22}\text{NaCl}$  (half-life = 950 days,  $\gamma$ -emitter,  $E_{\text{max}} = 511 \text{ keV}$ , PerkinElmer Radiochemicals). The PDADMA/PSS was soaked in 3 mL of the 0.1 M  $^{22}\text{NaBr}$  for 24 h in a flat-bottom sealed plastic tube. After doping, the solution was removed (and put aside to be reused for the next doping steps) and the tablet was quickly dabbed dry and weighed. The tube containing the tablet was placed in a well drilled into a plastic scintillator (SCSN-81, Kuraray, 12 mm thick, 38 mm x 38 mm area), which was in good optical contact with the fused silica window of an end-on RCA 8850 photomultiplier tube (PMT) powered at -2300 V. The PMT was connected to a frequency counter (Philips PM6654C) with a 10 s gate time and a -20 mV pulse threshold. The tablet was counted for at least 15 min. The tablet was then soaked in the  $^{22}\text{NaBr}$  solution with a higher concentration (by adding solid unlabeled NaBr to the reserved hot solution to go from 0.1 to 0.2 M NaBr), and the same equilibration and counting steps were repeated. A calibration curve was collected by placing aliquots of the  $^{22}\text{Na}$  labeled 0.1 M NaBr solution in the plastic tube and counting with the plastic scintillator. The background count rate was about 24 counts per second (cps). The count rate for the doped PEC was about 250 cps and counts were acquired for 7 min for a total of about  $10^5$  counts, which give a counting error of 0.3%.

**Ion Diffusion Coefficients by Self-Exchange.** The kinetics of diffusion were investigated in water and formamide-swelled PECs using  $^{22}\text{Na}$ -labeled sodium as a radiotracer. An 8 mm PDADMA/PSS tablet, of thickness about 1 mm, was immersed in a 0.4 M NaBr solution of either water or formamide, then dabbed dry with a lab wipe and immersed for 48 h in 4 mL 0.4 M NaBr solution spiked with 2  $\mu\text{Ci}$   $^{22}\text{Na}^+$  to reach equilibrium. The tablet was carefully dabbed dry again to remove any liquid on the surface and placed into 4 mL a solution of unlabeled 0.4 M NaBr (the

start of the experiment). Under constant, brisk stirring,  $^{22}\text{Na}^+$  in the PEC was self-exchanged with unlabeled  $\text{Na}^+$  in solution.

Aliquots of 100  $\mu\text{L}$  of the exchanging solution were withdrawn at various time points and mixed with liquid scintillating cocktail (Ecolite, MP Biochemicals) and counted in a Charm II counter (Charm Sciences). Three measurements at each time point were averaged. This experiment requires a data point at sufficiently long time,  $t = \infty$ , such that the exchange is complete. 48 h was used for this time. A data point taken 24 h later had the same count rate, showing 48 hours was sufficient for complete exchange. Counts for each sample ranged from about 5,000 to 40,000, with counting errors ranging from  $\pm 0.5$  to 1%.

## Results and Discussion

Two PEC compositions with  $T_g$  greater than room temperature when fully hydrated were selected to compare the plasticizing effectiveness of formamide relative to water. PDADMA/PSS has been studied extensively and is known to have a  $T_g$  of around 39 °C in aqueous solutions of low salt concentration.<sup>43</sup> In contrast, poly(vinylbenzyltrimethylammonium), PVBTA, complexed with PSS has a much higher  $T_g$  when fully hydrated, estimated to be about 102 °C.<sup>43</sup> Sulfonates can undergo an amidation reaction in the presence of formamide at low pH to form sulfonamides.<sup>44–46</sup> Figure S1 (Supporting Information) shows that the sulfonates within PVBTA/PSS are stable in formamide under the conditions used.

### Salt Resistance

The stability of pairing between  $\text{Pol}^+$  and  $\text{Pol}^-$  is commonly assessed using one of two methods. In the classical “salt resistance” concept, introduced by Bungenberg de Jong,<sup>8</sup> the salt concentration is increased until the PEC dissolves, at which point it is assumed all  $\text{Pol}^+\text{Pol}^-$  pairs are broken.<sup>41, 47–48</sup> The point of dissolution is identified approximately by visual observation (a cloudy solution becomes clear) or more accurately by turbidimetry (absorbance  $\rightarrow 0$ ). Static and dynamic light scattering are more sensitive methods to reveal aggregates in solutions that appear to be transparent.<sup>49</sup> The salt resistance is assumed to be near the CSC and the terms are used interchangeably here. Alternatively, the strength of  $\text{Pol}^+\text{Pol}^-$  pairing may be determined by following the amount of salt internally “doped” into the polymer at equilibrium as a function of external solution salt concentration.<sup>50</sup> The salt doping method is preferred, as salt resistance depends mildly on molecular weight<sup>51</sup> and PECs tend to be “inflated” with a high concentration of unbound co-ions near the CSC.<sup>52</sup> In addition, some PECs do not yield a CSC under experimentally accessible conditions.<sup>41</sup> For example, PDADMA/PSS cannot be dissolved in aqueous solutions of NaCl.<sup>53</sup> This was also found to be the case for PVBTA/PSS. In such examples, aqueous CSCs are sometimes attainable with the use of a more hydrophobic selection of ions along the Hofmeister series.

The CSC was measured either by increasing the [salt] until a suspension of PEC particles clarified or by adding pure solvent (thus decreasing the [salt]) until the solution became turbid. These techniques are respectively termed the “forward” and the “reverse” method. If there are no kinetic or thermodynamic limitations at the CSC, both methods should yield approximately the same results.<sup>26</sup> The two methods are less likely to superimpose for wide molecular weight distributions,<sup>26</sup> as used here, but they both intercept the concentration axis at the same points (Figure 1).

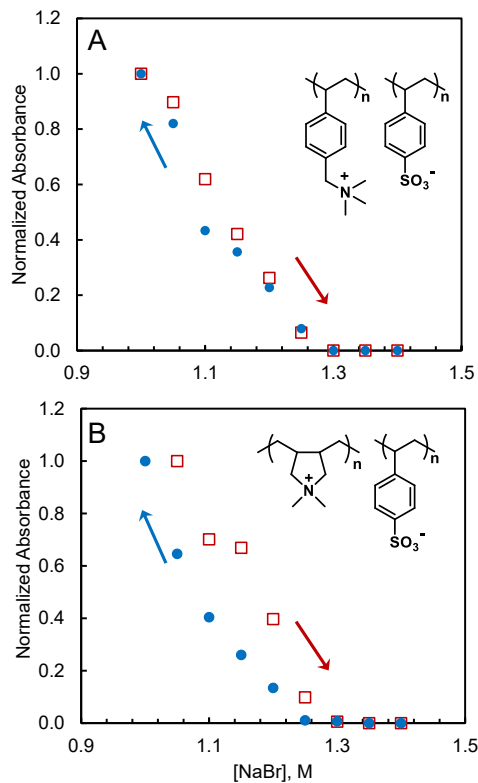


**Figure 1.** Turbidimetry to detect the dissociation of  $\text{Pol}^+\text{Pol}^-$  at the critical salt concentration at room temperature. Normalized absorbance at 390 nm of a PEC suspension *versus* the concentration of NaBr. Forward (red square) and reverse (blue circles) methods.

For PDADMA/PSS, shown in Figure 1, the CSC in formamide occurs at 1.3 M NaBr compared to 2.6 M NaBr in water.<sup>41</sup> The CSC of PVBTA/PSS is also about 1.3 M NaBr in formamide while it cannot be dissolved in aqueous NaBr.<sup>54</sup> CSC results for both PECs imply weaker binding between  $\text{Pol}^+$  and  $\text{Pol}^-$  in formamide than in water.

#### Enthalpies of Swelling and Complexation

The ionic nature of PECs provides them with such a strong affinity for water that they have recently been investigated as desiccants, outperforming state-of-the-art molecular sieves in some cases.<sup>42</sup> The affinity of PECs for a solvent may be ranked by comparing their relative enthalpies of swelling,  $\Delta H_{\text{swell}}$ .<sup>42</sup> These enthalpies were determined *via* solution calorimetry, where a known mass of dry PEC was immersed in the solvent of interest and the temperature change recorded. It was essential to dry the PECs by heating them (here to 120 °C) and immediately moving them to the drybox before they cooled. In our experience, PECs that are nominally “dry” in ambient conditions contain about 10 wt% water, as do the individual polyelectrolytes used to make them. The term “enthalpy of swelling” is used here to denote the heat change from the equilibrium uptake of solvent by dry, pure PEC (the reference state). In comparison, the terms enthalpy of solution and enthalpy of hydration commonly refer to dissolving a dry material to infinite dilution in solvent or transferring isolated species of a solute from the gas phase to water, respectively. For charged species, the latter can be quite exothermic.  $\Delta H_{\text{swell}}$  has previously been used to measure the hydration of dry crosslinked gels.<sup>55</sup>

Examples of the solution calorimetry are shown in Figure 2.  $\Delta H_{\text{swell}}$  for PDADMA/PSS in water and formamide were -137 and -128 J g<sup>-1</sup>, respectively; and for PVBTA/PSS  $\Delta H_{\text{swell}}$  was -85 J g<sup>-1</sup> in water compared to -127 J g<sup>-1</sup> in formamide. These exothermic values reveal strong specific

interactions of PECs with these two polar solvents, which is a result of the strong radial electric fields from the polyelectrolyte charges (i.e. the Born theory of solvation<sup>56</sup>). Most theories of PEC formation do not consider the energetics of the  $\text{Pol}^+\text{Pol}^-$  hydration shell, although Salehi and Larson<sup>57</sup> approximated Born solvation with a linear mixing rule for the effective dielectric constant. In addition to the Born solvation energy, smaller  $\Delta H_{\text{swell}}$  contributions are expected from van der Waals interactions of other parts of the polymers with water. While nominally “hydrophobic,” these parts may actually contribute small *exothermic* quantities.<sup>58</sup>

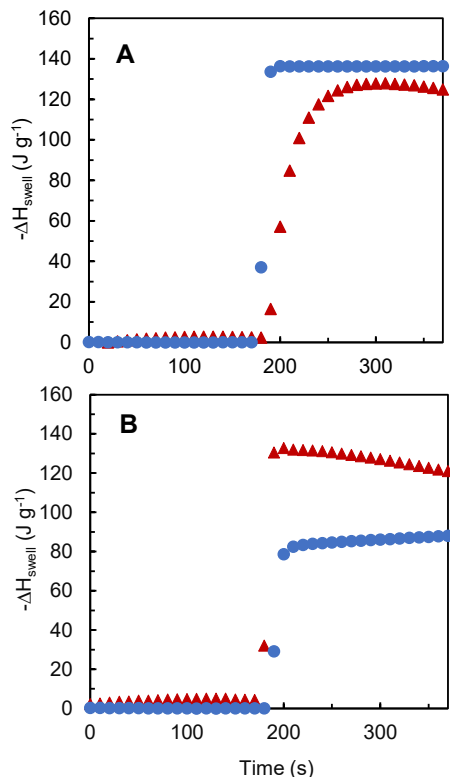


**Figure 2.** Calorimetry of PECs to determine the enthalpy of swelling. Temperature increases of less than 1 K at room temperature, measured when dry PEC powder was immersed in the solvent, were converted to J of released heat per g. **A**, PDADMA/PSS in water (blue circles), and formamide (red triangles). **B**, PVBTA/PSS in water (blue circles) and formamide (red triangles.) Data for PECs in water from reference 42.

Figure 2 shows that swelling of the same  $< 100 \mu\text{m}$  particle size of both PECs occurs more slowly in formamide. Using Chem3D version 20.0, the Connolly solvent excluded volume of water was  $10.3 \text{ \AA}^3$  and that for formamide was  $35.3 \text{ \AA}^3$ , which would explain the slower diffusion of formamide into the dried PEC. The volume of formamide is below the apparent PEC mesh size cutoff<sup>28</sup> for swelling of about  $50 \text{ \AA}^3$ . Chem3D also returned similar octanol-water partition coefficient of  $\log P = -1.38$  and  $-1.51$  for water and formamide, respectively.

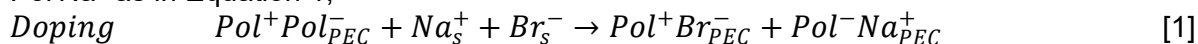
Enthalpies of complexation of polyelectrolytes in water solutions are typically small, sometimes unmeasurably so, which prompted Michaels to conclude that the entropy of counterion release was the driving forces for formation of PECs.<sup>2</sup> This omnipresent driving force is supplemented by small enthalpic contributions (endo- or exothermic), mainly attributed to changes in the solvation environment of charges.<sup>59</sup> Isothermal titration calorimetry revealed small enthalpies of complexation,  $\Delta H_{\text{PEC}}$ , in both water and formamide (see Supporting Information Figure S2 for ITC thermograms), summarized in Table 1. Enthalpies of complexation are less

negative in formamide than in water. However, the differences are small despite a factor of 1.4 difference in dielectric constant.

**Table 1.** Enthalpies of complexation for polyelectrolytes in water and formamide at 25 °C. All experiments were conducted with PSSNa as polyanion and a salt concentration of 0.01 M NaBr.

Polycation	Solvent	$\Delta H_{PEC}$ (+/- 100) J mol <sup>-1</sup>
PDADMA(Br)	Water	-1200
PDADMA(Br)	Formamide	85
PVBTA(Br)	Water	-520
PVBTA(Br)	Formamide	-160

In doping experiments, salt MA, such as NaBr, added to solution enters the PEC in a reversible manner and breaks a fraction,  $y$ , of  $\text{Pol}^+\text{Pol}^-$  pairs, forming extrinsic sites  $\text{Pol}^+\text{Br}^-$  and  $\text{Pol}^-\text{Na}^+$  as in Equation 1,<sup>58</sup>



where the subscript “PEC” refers to the PEC phase and “s” to the solution phase. Equation 1 implies that all MA that dopes a PEC breaks  $\text{Pol}^+\text{Pol}^-$  pairs and become counterions for their respective polyelectrolyte repeat units, but only a fraction,  $f$ , which decreases with increasing doping, actually do so, the rest occupying space within the PEC as co-ions.<sup>57-58</sup> The ratio,  $r$ , between the total salt and total polyelectrolyte concentration,  $[\text{PE}]_{PEC}$ , within the PEC is,<sup>58</sup>

$$r = \frac{[\text{MA}]_{PEC}}{[\text{PE}]_{PEC}} \quad [2]$$

Thus,  $y = fr$ . The equilibrium for unpairing in Equation 1 is represented<sup>58</sup> by a constant  $K_{unp}$

$$K_{unp} = \frac{y^2[\text{PE}]_{PEC}}{(1-y)[\text{MA}]_{PEC}} \quad [3]$$

An approximation for  $K_{unp}$  using the molar volume of the PEC,  $V_m$  ( $= \frac{1}{[\text{PE}]_{PEC}}$ ), is<sup>58</sup>

$$K_{unp} \approx f_0^2 V_{m,0} e^{\frac{f_0 \Delta H_{PEC}}{RT}} \quad [4]$$

where  $f_0$  is the value of  $f$  at low doping levels (e.g.  $y$  is less than 0.1 or 10%) and  $V_{m,0}$  is the molar volume at these levels. Unfortunately, it is difficult to estimate  $f$ , other than by computational methods<sup>57</sup>, though  $f$  tends to increase at low doping levels.<sup>60</sup> In Figure 3A it is seen that  $r$  as a function of  $[\text{NaBr}]_s$  is almost identical for water and formamide.  $V_{m,0}$  is about 0.45 L mol<sup>-1</sup> and about 0.53 L mol<sup>-1</sup> for PDADMA/PSS in water and formamide, respectively, assuming 40 wt% water and 51 wt% formamide and a dry PDADMA/PSS density of 1.26 g cm<sup>-3</sup>.<sup>28</sup> This means the other factors,  $f_0$  and  $\Delta H_{PEC}$ , compensate each other and the doping curves turn out to be similar (Figure 3A).

The distribution of ions in solution *versus* in the stoichiometric PEC is given by the following equilibrium,<sup>58</sup>

$$[\text{NaBr}]_{PEC} = [\text{NaBr}]_s e^{\frac{f \Delta H_{PEC}}{2RT}}. \quad [5]$$

If  $\Delta H_{PEC} \approx 0$ , Equation 5 predicts  $[\text{NaBr}]_{PEC} = [\text{NaBr}]_s$ , which is almost found experimentally (Figure 3B). The small intercepts on the  $[\text{NaBr}]_s$  axes in Figure 3 are from a small amount of polyelectrolyte nonstoichiometry and the osmotic pressure generated by the polyelectrolyte chain network in the PEC.<sup>28</sup> The volume of the PEC remained constant ( $\pm 2\%$ ) with doping in formamide over the range studied in Figure 3, while in water the volume increased by 9% over the same range.<sup>60</sup>

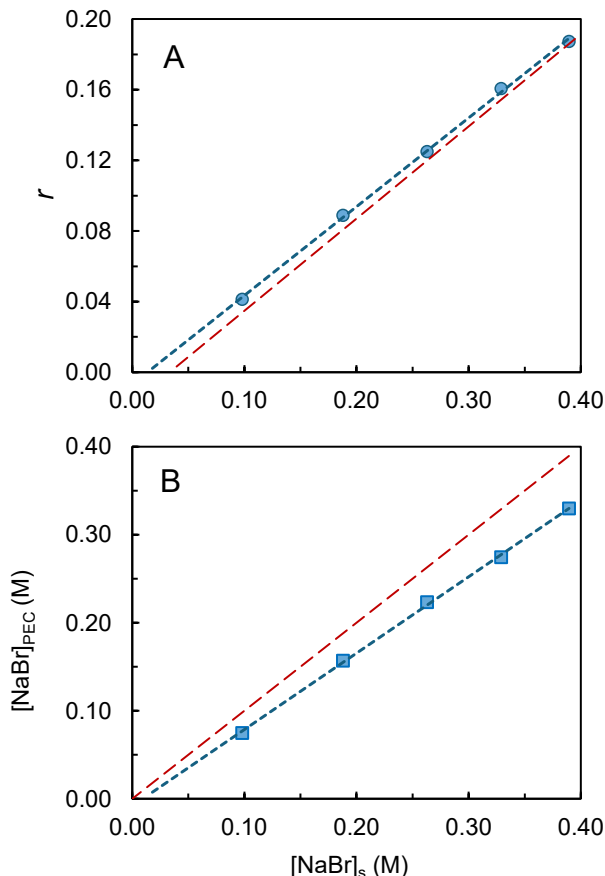


**Figure 3.** Doping of PDADMA/PSS by NaBr in formamide. **A**; the doping level,  $r$ , is the molar ratio of NaBr:polyelectrolyte within the PEC. The red long-dashed line corresponds to doping of the same PEC by the same salt in water (from reference 60). **B**; the concentration of NaBr in the PEC,  $[\text{NaBr}]_{PEC}$ , versus the concentration in the solution,  $[\text{NaBr}]_s$ . The long-dashed line is theoretical using Equation 5 assuming athermal doping, where  $[\text{NaBr}]_{PEC} = [\text{NaBr}]_s$ . Short-dashed lines are linear least squares fit to the data. The precision of each data point is  $\pm 4\%$  and accuracy is  $\pm 10\%$ .

If they are used to compare  $\text{Pol}^+\text{Pol}^-$  pairing strengths, the close doping responses for PDADAMA/PSS between NaBr in water and formamide shown in Figure 3A contradict the significantly greater difference in concentrations (respective CSCs of 2.6 M versus 1.3 M) needed to dissociate the PEC in these solvents. It has been noted that it may be difficult or impossible to achieve a CSC with a particular salt for PECs that exhibit *exothermic*  $\Delta H_{PEC}$ .<sup>41</sup> The rationale for this observation is that  $\Delta H_{PEC}$  provides a measure of differences in specific interactions between  $\text{Pol}^+$  and  $\text{Pol}^-$  as pairs and as their respective counterion-compensated forms  $\text{Pol}^+\text{A}^-$  and  $\text{Pol}^-\text{M}^+$ . An endothermic  $\Delta H_{PEC}$  implies that counterions, on average, prefer to break  $\text{Pol}^+\text{Pol}^-$  pairs while

an exothermic  $\Delta H_{PEC}$  implies that counterions prefer to act as co-ions within the PEC and not break  $\text{Pol}^+\text{Pol}^-$  pairs.<sup>41</sup> Thus, PECs with more exothermic  $\Delta H_{PEC}$  must be pressed to higher [salt] to break all  $\text{Pol}^+\text{Pol}^-$  pairs and reach the CSC. A good example is provided by the much-studied PDADMA/PSS, which has a CSC of 1.8 M in KBr ( $\Delta H_{PEC} \approx 0$ ) whereas simply changing  $\text{K}^+$  for  $\text{Na}^+$  ( $\Delta H_{PEC} = -1200 \text{ J mol}^{-1}$ ) pushes the CSC to 2.6 M in NaBr. Because  $\Delta H_{PEC}$  of PDADMA/PSS and PVBTA/PSS in formamide are close and nearly athermal (Table 1), their CSCs (Figure 1) are similar and measurable at experimentally achievable [salt]. Reliable comparisons of the CSC or salt resistance between different PECs are best made under athermal ( $\Delta H_{PEC} \approx 0$ ) conditions.  $\Delta H_{PEC}$  is adjusted by the choice of counterions.<sup>60</sup>

### Solvent Composition

Previous work has shown that the few solvents that swell PECs do so to different extents.<sup>28</sup> The solvent content of the PEC as a function of solution composition was determined using ATR-FTIR. PECs equilibrated in solvent were squashed against a single-bounce diamond ATR crystal. The vibrational bands corresponding to formamide and water overlapped, so  $\text{D}_2\text{O}$  was used in place of  $\text{H}_2\text{O}$  to give well-separated bands (Figure 4 and Supporting Information Figures S3 and S4). In prior work with  $\text{H}_2\text{O}/\text{D}_2\text{O}$  mixed solvents there was less than 3% preference of  $\text{H}_2\text{O}$  compared to  $\text{D}_2\text{O}$  in swelling PDADMA/PSS.<sup>61</sup> Solutions of known concentrations of PSS in formamide and PSS in  $\text{D}_2\text{O}$  provided calibration curves (Supporting Information Figure S4) to convert the ratio of respective peak areas in PECs to the mole ratio.

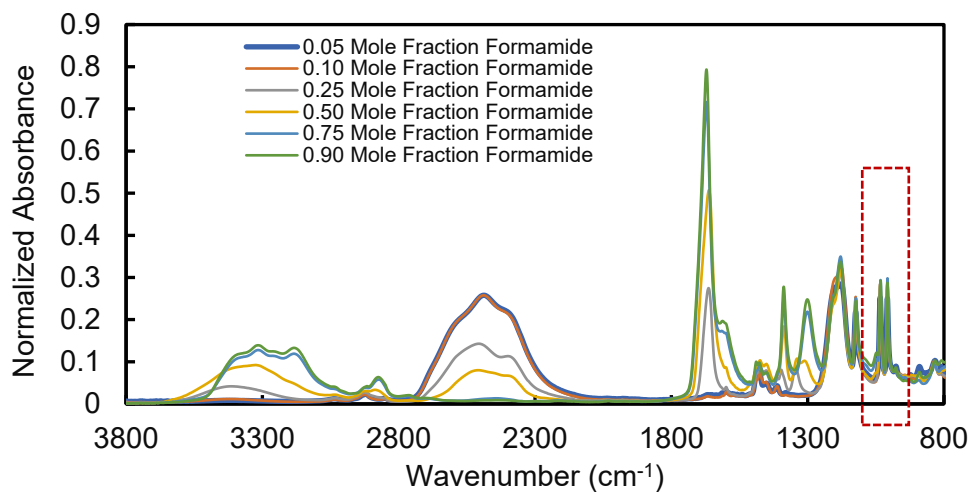


**Figure 4.** ATR-FTIR of PDADMA/PSS in  $\text{D}_2\text{O}$ /formamide mixtures. Strong features are from the O-D stretch at  $2500 \text{ cm}^{-1}$  and C=O stretching from formamide at  $1670 \text{ cm}^{-1}$ . Dotted box shows PSS reference peaks. Samples were allowed to equilibrate in solvents at room temperature for 24 h before measurements.

Figure 5 shows that the content of a particular solvent with PDADMA/PSS PEC is approximately proportional to its mole fraction in the external bathing medium. The total number of solvent molecules per  $\text{Pol}^+\text{Pol}^-$  pair remains roughly constant at  $6 \pm 0.8$ . Solvation by water is slightly favored over solvation by formamide (the enthalpy of PEC solvation for the former is slightly higher in Figure 2).

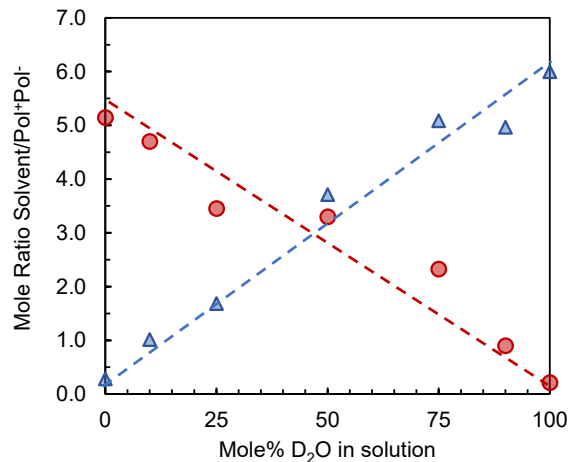


**Figure 5.** FTIR composition of solvents within PDADMA/PSS as a function of the mole fraction of solvent in the bath. Room temperature. The composition is given as the ratio of solvent molecules to  $\text{Pol}^+\text{Pol}^-$  pairs. Error is  $\pm 0.8$  solvent/ $\text{Pol}^+\text{Pol}^-$ .

PDADMA/PSS equilibrated in 0.01 M NaBr in formamide for 1 month contained 51% by weight of solvent (volume fraction 54% assuming a PDADMA/PSS density of  $1.26 \text{ g cm}^{-3}$ ), which is about 7 formamide molecules per  $\text{Pol}^+\text{Pol}^-$ , somewhat more than about 5 molecules presented in Figure 5. It is believed that this difference is due to the pressure (several atmospheres) which was used to squash the PEC against the ATR crystal. Loosely bound solvent would be pressed out of the PEC, as it is under osmotic pressure.<sup>12</sup> Similarly, from Figure 5, the water content of PDADMA/PSS in pure water was about 6  $\text{H}_2\text{O}$  per  $\text{Pol}^+\text{Pol}^-$ , which is lower than about 10  $\text{H}_2\text{O}$  (37 weight%, 42% volume fraction) per  $\text{Pol}^+\text{Pol}^-$  in unpressed PEC.<sup>60</sup> Batys et al. found,<sup>25</sup> using differential scanning calorimetry, that 29.1 wt% water, or about 7  $\text{H}_2\text{O}$  per  $\text{Pol}^+\text{Pol}^-$ , in PDADMA/PSS was nonfreezing, attributed to strong binding. Presumably, these water molecules would resist being expelled from the PEC by hydrostatic pressure.

#### PEC Dynamics in Formamide

Variable temperature rheology measurements of the two PECs in water or formamide were performed in order to investigate their influence on  $T_g$ , located by the peak of  $\tan\delta$ . In addition, the proportions of solvent in the rheometer reservoir, and therefore the proportions of solvent in the PEC according to Figure 5, were varied. Compositions are based on mole fractions, also expressed as mole percentages. All solutions had 0.01 M NaBr to prevent possible spontaneous inflation and pore formation induced by the residual osmotic pressure in the PEC.<sup>28</sup>

PDADMA/PSS in water exhibited a  $T_g$  of  $37^\circ\text{C}$  as seen in Figure 6, which agrees with the literature.<sup>43</sup> The addition of even a small amount of formamide decreased the  $T_g$ ; for example, solution compositions of 5 mol% to  $21^\circ\text{C}$ , and 10 mol% to  $6^\circ\text{C}$  (see Figure 6B and 6C). Further additions of formamide moved  $T_g$  out of the temperature scan range (Figure 6E). The PVBTA/PSS PEC was particularly useful for demonstrating the strong shift in  $T_g$  with the addition of formamide (Figure 7). In pure water  $T_g$  was slightly above  $100^\circ\text{C}$  (estimated to be  $102^\circ\text{C}$  in previous work<sup>43</sup>). In formamide, the  $T_g$  was lowered by about 75 degrees to  $27^\circ\text{C}$  (Figure 7).

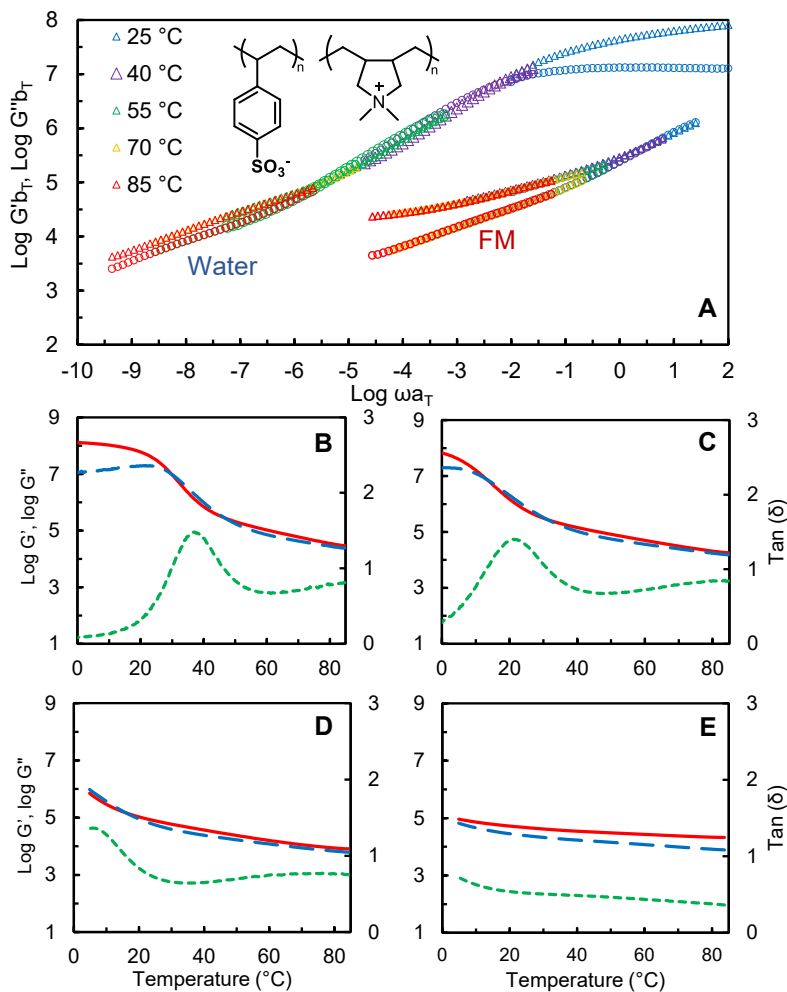


**Figure 6.** **A**, time-temperature (see inset) superposition (TTS) of the LVR of PDADMA/PSS in water, upper curves, and formamide (FM), lower curves (both with 0.01 M NaBr). Triangles correspond to storage modulus  $G'$ , circles correspond to loss modulus  $G''$ , in Pa. Frequency in  $\text{rad s}^{-1}$ . Reference temperature was 25 °C. Shift factors provided in Supporting Information Figure S5. **B - E**,  $G'$  (solid line),  $G''$  (long dash line) and  $\tan(\delta)$  (short dash line) versus temperature (cooling ramps at 0.1 Hz) of PDADMA/PSS in various mole fractions of formamide in water (0.01 M NaBr for all solutions): **B**, 0.00 formamide; **C**, 0.05 formamide; **D**, 0.10; **E**, 1.00. Additional compositions provided in Supporting Information Figure S6.

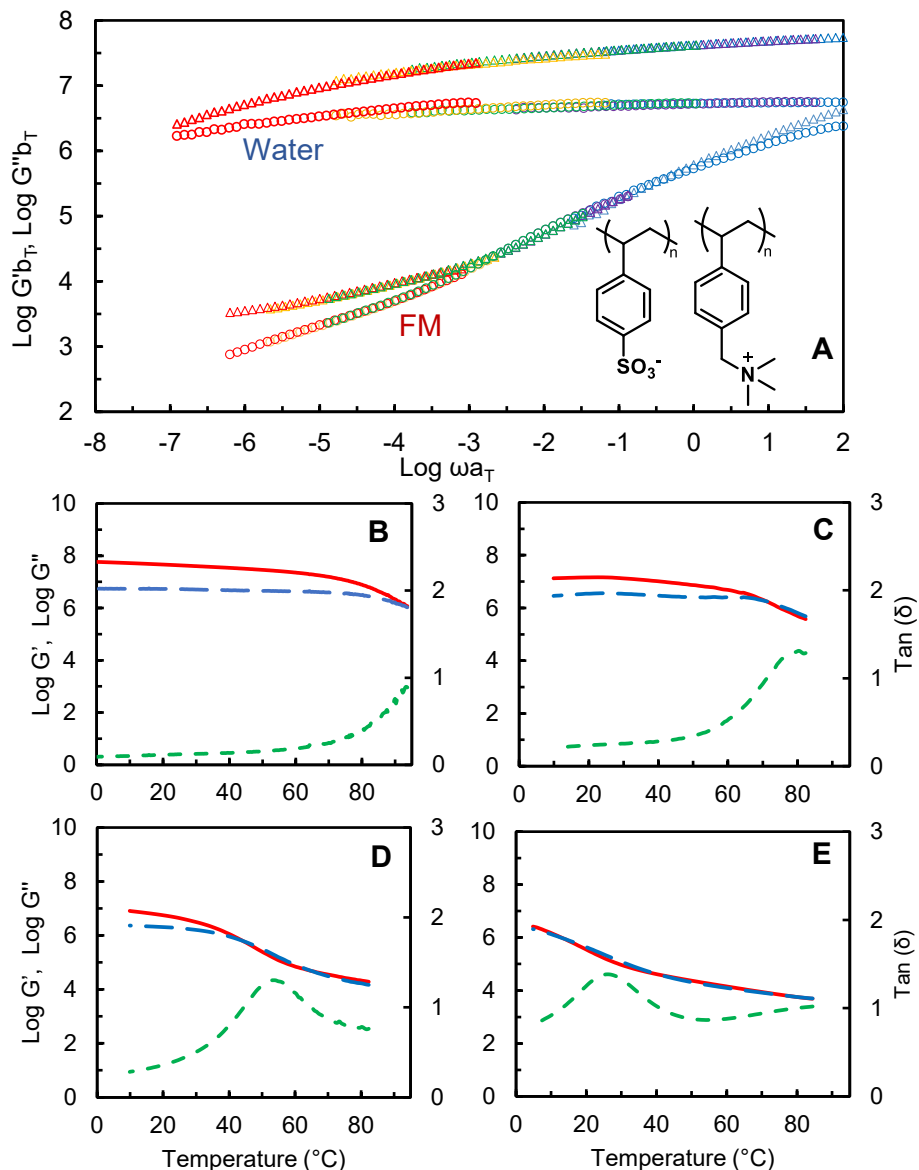


**Figure 7.** **A**, TTS of PVBTA/PSS in water, upper curves, and formamide (FM), lower curves (both with 0.01 M NaBr). Triangles correspond to  $G'$ , circles correspond to  $G''$ , Pa. Frequency in  $\text{rad s}^{-1}$ . Reference temperature was 25 °C. Shift factors provided in Supporting Information Figure S7. **B - E**,  $G'$  (solid line),  $G''$  (long dash line) and  $\tan(\delta)$  (short dash line) (cooling ramps at 0.1 Hz) of PVBTA/PSS in various mole fractions of formamide with 0.01 M NaBr: **B**, 0.00; **C**, 0.10; **D**, 0.25; **E**, 1.00. Additional compositions provided in Supporting Information Figure S8.

Frequency sweep experiments for both PECs in 100% water and 100% formamide, with 0.01 M NaBr added, were performed from 0.1 to 100  $\text{rad s}^{-1}$  at multiple temperatures and stitched together in Figures 6 and 7 by using time-temperature superposition (TTS) and shift factors (horizontal,  $a_T$ , vertical,  $b_T$  summarized in Figures S5 and S7).

Strong plasticization by formamide relative to water is demonstrated in Figures 6 and 7. Quantitative comparisons of relaxation times versus temperature are difficult because different sets of shift factors are employed for each solvent. Also, the temperature span goes through the  $T_g$  of PDADMA/PSS in water and through the  $T_g$  of both PECs at different temperatures when

immersed in mixed solvents (see Figures 6 B-E and 7 B-E). Further, the polyelectrolytes have a broad molecular weight distribution, which would complicate detailed analysis of the relaxation versus frequency, often performed for polymers of narrow polydispersity considerably above their  $T_g$ .<sup>62</sup> The scaling of 2 and 1 in the terminal regime for  $G'$  and  $G''$  respectively is not seen here because  $\omega_{aT}$  does not go to low enough frequencies, whereas it is observed in narrow molecular weight distribution liquidlike PECs.<sup>26</sup>

Notwithstanding these limitations, various types of superpositions have been attempted for PECs, such as time-salt superposition and time-water superposition, exploiting the plasticizing effects of salt doping and water content.<sup>63</sup> Attempts to obtain a master curve combining the responses in water and formamide are shown in Figure 8. Frequencies for the entire formamide curve were all shifted by a constant factor  $k_s$ . The solvent superposition master curve for PDADMA/PSS required a  $b_s$  shift and was not satisfactory at lower frequencies for unknown reasons. The PVBTA/PSS in formamide data provided reasonable master curves with  $k_s = 2 \times 10^{-9}$  and no  $b$ -shifting. These master curves show the effective chain dynamics of PDADMA/PSS and PVBTA/PSS at a particular reference temperature near  $T_g$  are accelerated when solvated by formamide instead of water. The exceptionally small values of  $k_s$  obtained here are because both systems go across a glass transition.

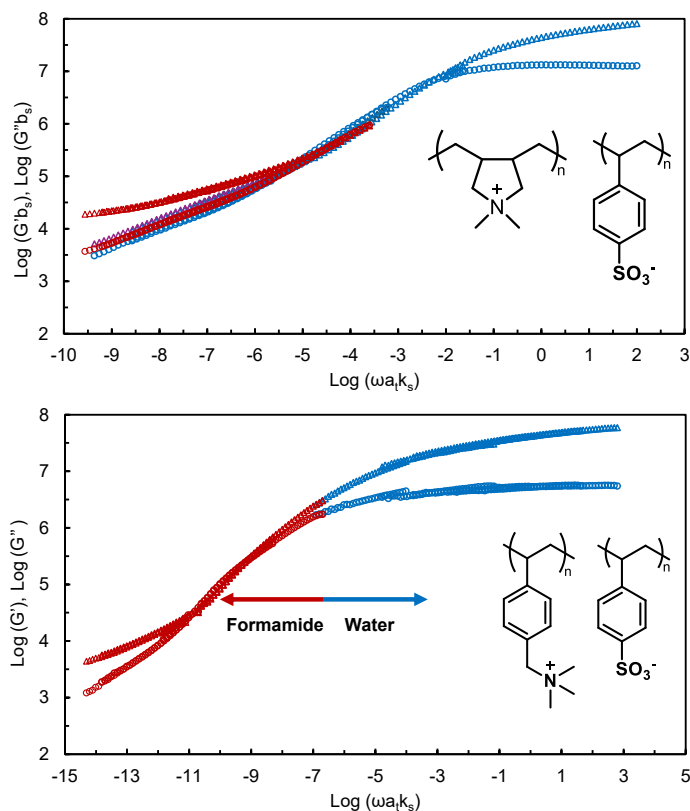


**Figure 8.** Attempted LVR “solvent master curve” by shifting all TTS in formamide by a factor  $k_s$  relative to water (i.e. reference solvent is water) on the frequency axis.  $G'$  and  $G''$  in Pa,  $\omega$  in rad s<sup>-1</sup>. **A**, for PDADMA/PSS ( $k_s = 10^{-5}$ ); and **B**, for PVBTA/PSS ( $k_s = 2 \times 10^{-9}$ ). Reference temperature = 25 °C.

It is reasonable to assume that stronger association between  $\text{Pol}^+$  and  $\text{Pol}^-$  would be correlated to slower dynamics and therefore stiffer materials. According to Equation 4, strength is related to volume charge density ( $= 1/V_m$ ) and  $f$ , which is, in turn, enhanced by endothermic  $\Delta H_{\text{PEC}}$ . The role of charge pairing in stabilizing biomaterials has long been debated in biomacromolecules. “Salt bridges” in proteins are formed by pairing of positively and negatively-charged amino acid residues.<sup>64–65</sup> Salt bridges can be found either “exposed” on the outer surface of the protein or “buried” within the protein.<sup>66</sup> Using a continuum electrostatics analysis, exposed salt bridges were suggested to contribute from 0 to 8  $\text{kJ mol}^{-1}$  additional structural stability while buried salt bridges contribute up to 13  $\text{kJ mol}^{-1}$ .<sup>67</sup> The computed strength of the buried salt bridges was attributed to a surrounding lower effective dielectric constant (from 4 – 37), compared to the dielectric constant surrounding the exposed salt bridge which approaches 80 (i.e. that of water).<sup>67–68</sup> Accordingly, a higher dielectric constant medium might be expected to weaken interactions between  $\text{Pol}^+$  and  $\text{Pol}^-$ . From Figure 3A this effect is weak. Figure 3B shows reasonable agreement between the experimental and calculated  $[\text{NaBr}]_{\text{PEC}}$  versus  $[\text{NaBr}]_s$  using Equation 5, which does not explicitly contain a dielectric constant (although  $\Delta H_{\text{PEC}}$  may include dielectric constant effects). Bosshard et al.<sup>66</sup> point out that solvation changes occurring when peptides pair to form salt bridges are a major contribution to the free energy change. In particular, desolvation (unfavorable) is expected to occur for buried salt bridges, rendering them destabilizing.<sup>66</sup> We have stressed the importance of changes in solvation environment on PEC formation, showing that the level of water hydrogen bonding disruption is proportional to  $\Delta H_{\text{PEC}}$ , and that athermal complexation may be interpreted as a zero net change in solvation shell enthalpy between  $\text{Pol}^+\text{Pol}^-$  versus  $\text{Pol}^+\text{A}^-$  and  $\text{Pol}^-\text{M}^+$ , leaving entropy as the sole driving force.<sup>26, 58, 59</sup>

The dynamics represented in Scheme 1 are at the pendant group level whereas the dynamics of a linear chain are represented theoretically by the relaxation time of a Kuhn length of the polymer backbone and, if they are entangled, by the segment length between entanglements.<sup>62</sup> We have used ion transport measurements to determine the lifetime of a  $\text{Pol}^+\text{Pol}^-$  pair, reasoning that the average ion diffusion coefficient  $D_{\text{ions}}$  depends on the average ion hopping rate  $\omega_{\text{ion}}$  between charged polyelectrolyte segments which is the same rate at which  $\text{Pol}^+\text{Pol}^-$  pairs are broken  $\omega_{\text{pair}}$ .<sup>26</sup>

$$\omega_{\text{ion}} = \omega_{\text{pair}} = \frac{6D_{\text{ions}}}{d^2} \quad [6]$$

where  $d$  is the average distance between  $\text{Pol}^+\text{Pol}^-$  pairs. The volume,  $V_m$ , of one mole of PDADMA/PSS in 0.4 M NaBr,  $520 \text{ cm}^3$ , was taken from prior work.<sup>60</sup>  $V_m$  for the same PEC in 0.4 M NaBr in formamide was  $350 \text{ cm}^3$ . Using  $d = \sqrt[3]{V_m/N_A}$ , where  $N_A$  is Avogadro’s number,  $d$  is 0.95 nm for water and 0.83 nm for the formamide-swelled PEC. In previous studies of PDADMA/PSS in water<sup>69</sup>  $D_{\text{ion}}$  exhibited almost no change when the PEC went through  $T_g$ , showing the dynamics of  $\text{Pol}^+\text{Pol}^-$  pair breaking are less cooperative than those of backbone motions. Such a property is sought in studies of ion conducting polymers for batteries.<sup>70</sup>

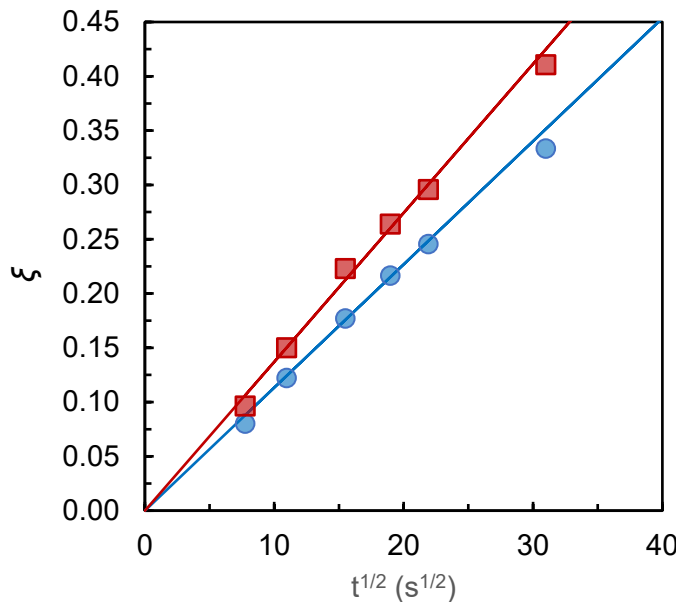


**Figure 9.** Fraction  $\xi$  of  $^{22}\text{Na}^+$  in PDADMA/PSS exchanged with unlabeled  $\text{Na}^+$  in 0.4 M NaBr solution versus time  $t^{1/2}$  at room temperature. Squares, in water; circles, in formamide. Solid lines are fits to Equation 7 using  $D_{\text{Na}^+} = 2.30 \times 10^{-6} \text{ cm}^2 \text{ s}^{-1}$  for water and  $D_{\text{Na}^+} = 1.45 \times 10^{-6} \text{ cm}^2 \text{ s}^{-1}$  for formamide. Samples were discs of PEC, thickness  $\sigma = 0.125 \text{ cm}$  for water, and  $0.120 \text{ cm}$  for formamide. Precision and accuracy of each data point is  $\pm 5 \%$ .

To compare the pair breaking rate for a PEC hydrated by water *versus* solvated by formamide,  $D_{\text{ion}}$  was measured *via* the self-exchange of radiolabeled  $^{22}\text{NaBr}$ . Similar samples of PDADMA/PSS were doped in 0.4 M  $^{22}\text{NaBr}$  in water or formamide, which, according to Figure 3, gives similar doping levels. Under stirring, the radiolabeled  $^{22}\text{Na}^+$  was allowed to self-exchange with unlabeled  $\text{Na}^+$  in unlabeled 0.4 M NaBr and the amount of released isotope was tracked by scintillation counting. If the fraction,  $\xi$ , of exchanged  $^{22}\text{Na}^+$  in the PEC as a function of time,  $t$ , is held below 0.6,  $\xi$  is given by<sup>26</sup>

$$\xi = \left( \frac{2\sqrt{D_{\text{ions}}t}}{\sigma\sqrt{\pi}} \right)_{\xi < 0.6} \quad [7]$$

where  $\sigma$  is the thickness of the PEC. In Figure 9,  $\xi$  is plotted *versus*  $t^{1/2}$ . The diffusion coefficients for PDADMA/PSS immersed in water and formamide were  $2.30 \times 10^{-6} \text{ cm}^2 \text{ s}^{-1}$  and  $1.45 \times 10^{-6} \text{ cm}^2 \text{ s}^{-1}$ , respectively. Using values of  $d$  for hydrated *versus* formamide-swelled PEC in 0.4 M NaBr the room temperature pair breaking rates  $\omega_{\text{pair}}$  (Equation 6) were  $1.5 \times 10^9 \text{ s}^{-1}$  and  $1.3 \times 10^9 \text{ s}^{-1}$ , respectively.

If  $\omega_{\text{pair}}$  is similar in water and formamide why are the  $T_g$ s in these solvents so different? Individual ion hopping/pair breaking events occur with minimal cooperativity whereas polymer backbone motions are highly cooperative. Ions that are “solvated” by polymer chain segments rely on the motion of these segments for mobility.<sup>71</sup> In contrast, pendant groups only need to swing less than 1 nm to transfer counterions to adjacent pendant groups. The dynamically relevant length of an ideal polymer segment is the Kuhn length, which has been shown to be about 10 repeat units in a related PEC.<sup>26</sup> The pair exchange mechanism in Scheme 1, which

allows polyelectrolytes in PECs to flow, is much slower than  $\omega_{\text{pair}}$ , e.g. on the order of 1  $\mu\text{S}$  per event at room temperature.<sup>26</sup> Five of these pair exchanges must occur to allow one Kuhn length to move. Thus, the level/range of cooperativity of the backbone motions are much greater than those of individual ions, leading to apparent decoupling of ion and backbone motions. Approaching  $T_g$ , the motions of the polymer backbone become increasingly cooperative/longer range, limited by free volume,<sup>72</sup> indicated by increasingly steeper changes in shift factor versus temperature, as seen in Supporting Information Figure S5A. Figure 6B (PDADMA/PSS in water) shows strong modulus changes near  $T_g$  (about 35 °C), a consequence of this increased cooperativity, whereas Figure 6E, the same PEC in formamide, depicts a flatter response since the material is far above  $T_g$ . To further illustrate this point, Figure S9 (Supporting Information) provides a zoom-in of higher temperature responses of  $G'$  in water compared to formamide. If the modulus is controlled by the pair breaking and exchange rate shown in Figure 1, the modulus of PEC in water or formamide should be comparable, all other things (such as molecular weight, ratio, and solvent volume fraction) being equal. Figure S9 suggests the modulii are indeed converging at higher temperatures.

Though there are about the same number of waters or formamides per  $\text{Pol}^+\text{Pol}^-$  (Figure 5), the formamide molecule is larger, which means the volume fraction is larger. Whether this additional volume is free volume, which shifts  $T_g$  lower, may also depend on where the solvent is located. The (hydrophobic) backbone may experience superior plasticization in formamide, because it is more solvated. Formamide is miscible with low-polarity solvents such as chloroform and ethyl ether.<sup>73</sup> Differential solvation of backbone and sulfonated pendant group is strong enough in Nafion to induce nanophase separation and segregation of sulfonates into ion-conducting channels.<sup>4</sup>

## Conclusions

Formamide, a potent plasticizer for polyelectrolyte complexes, significantly reduces PEC glass transition temperatures compared to those found in water-swelled systems. PDADMA/PSS, a common and widely-studied example of a PEC with  $T_g$  above room temperature, takes up about the same amounts of water and formamide at equilibrium. Mixing a small amount of formamide into an aqueous solution lowers the  $T_g$  and full plasticization, according to the LVR, is observed at a formamide content of about 50%. Equilibrium composition studies show no significant preference for swelling by water or formamide in terms of number of molecules per  $\text{Pol}^+\text{Pol}^-$  repeat, but the volume fraction of formamide in PECs is greater.

Though toxic, formamide provides insight on the role of small-molecule swelling agents, notably water, on the properties of PECs. An equilibrium expression accurately predicted the distribution of salt ions between solution and PEC. Ion transport, reflecting the hopping of ions between neighboring charged sites in the PEC, occurs at a similar rate at room temperature in water-swelled PEC (below  $T_g$ ) as in the formamide counterpart (above  $T_g$ ). These similarities in ion transport were observed despite differences in dielectric constant, raising questions regarding the transition state depicted in Scheme 1. However, while dielectric constants are known in bulk solutions, the effective dielectric constant between charges for PECs in water relative to formamide is unknown and may be much less than the bulk values for these solvents.

Liquidlike PECs, or coacervates, already exhibit far more chain mobility than the glassy PECs studied here. For researchers interested in coacervate droplets as artificial cells,<sup>7-8, 51</sup> combinations of polyelectrolytes exhibiting solid-like properties can be liquified with the addition of formamide. The dielectric constant of methylformamide (MF), 180, is even higher than that of formamide and MF is less toxic. Unfortunately, the PECs studied here were not swelled by MF, although mixtures of MF and other solvents might be able to swell PECs. Our prior work points to a sharp cutoff in size for swelling of PECs by small molecules.<sup>28</sup>

## Supporting Information

Stability of PSS in formamide, isothermal calorimetry of polyelectrolyte complexation, ATR-FTIR spectra of water/formamide mixtures in PDADMA/PSS, shift factors for PECs in water and formamide linear viscoelasticity, LVR versus temperature for PECs in pure and mixed solvents.

## Notes

The authors declare no competing financial interest.

## Acknowledgment

This research was sponsored by the Department of the Navy, Office of Naval Research, award N00014-23-1-2125, and by the National Science Foundation, grant DMR 2103703.

## References

1. Wypych, G., *Handbook of Plasticizers*. ChemTec Publishing: 2004.
2. Wiesinger, H.; Bleuler, C.; Christen, V.; Favreau, P.; Hellweg, S.; Langer, M.; Pasquettaz, R.; Schönborn, A.; Wang, Z., Legacy and Emerging Plasticizers and Stabilizers in PVC Floorings and Implications for Recycling. *Environmental Science & Technology* **2024**, *58*, 1894-1907.
3. Chandran, P. L.; Horkay, F., Aggrecan, an Unusual Polyelectrolyte: Review of Solution Behavior and Physiological Implications. *Acta Biomater* **2012**, *8*, 3-12.
4. Kusoglu, A.; Weber, A. Z., New Insights into Perfluorinated Sulfonic-Acid Ionomers. *Chemical Reviews* **2017**, *117*, 987-1104.
5. Michaels, A. S., Polyelectrolyte Complexes. *Journal of Industrial and Engineering Chemistry* **1965**, *57*, 32-40.
6. Bixler, H. J.; Michaels, A. S., Polyelectrolyte Complexes. In *Encyclopedia of Polymer Science and Technology*, Interscience: New York, 1969; Vol. 10, pp 765-80.
7. Bungenberg de Jong, H. G.; Kruyt, H. R., Coacervation (Partial Miscibility in Colloid Systems). *Proc. Koninkl. Med. Akad. Weterschap.* **1929**, *32*, 849-856.
8. Bungenberg de Jong, H., in *Colloid Science*, Vol. 2, Kruyt, H.R., Ed. *Amsterdam, Elsevier* **1949**, *1*, 0.
9. Schönhoff, M.; Ball, V.; Bausch, A. R.; Dejugnat, C.; Delorme, N.; Glinel, K.; Von Klitzing, R.; Steitz, R., Hydration and Internal Properties of Polyelectrolyte Multilayers. *Colloids Surf. A* **2007**, *303*, 14-29.
10. Decher, G., Fuzzy Nanoassemblies: Toward Layered Polymeric Multicomposites. *Science* **1997**, *277*, 1232-1237.
11. Pavoort, P. V.; Bellare, A.; Strom, A.; Yang, D. H.; Cohen, R. E., Mechanical Characterization of Polyelectrolyte Multilayers Using Quasi-Static Nanoindentation. *Macromolecules* **2004**, *37*, 4865-4871.
12. Hariri, H. H.; Lehaf, A. M.; Schlenoff, J. B., Mechanical Properties of Osmotically Stressed Polyelectrolyte Complexes and Multilayers: Water as a Plasticizer. *Macromolecules* **2012**, *45*, 9364-9372.

13. Francius, G.; Hemmerle, J.; Ball, V.; Lavalle, P.; Picart, C.; Voegel, J. C.; Schaaf, P.; Senger, B., Stiffening of Soft Polyelectrolyte Architectures by Multilayer Capping Evidenced by Viscoelastic Analysis of AFM Indentation Measurements. *J Phys Chem C* **2007**, *111*, 8299-8306.
14. Nolte, A. J.; Cohen, R. E.; Rubner, M. F., A Two-Plate Buckling Technique for Thin Film Modulus Measurements: Applications to Polyelectrolyte Multilayers. *Macromolecules* **2006**, *39*, 4841-4847.
15. Trenkenschuh, K.; Erath, J.; Kuznetsov, V.; Gensel, J.; Boulmedais, F.; Schaaf, P.; Papastavrou, G.; Fery, A., Tuning of the Elastic Modulus of Polyelectrolyte Multilayer Films Built up from Polyanions Mixture. *Macromolecules* **2011**, *44*, 8954-8961.
16. Nolte, A. J.; Rubner, M. F.; Cohen, R. E., Determining the Young's Modulus of Polyelectrolyte Multilayer Films Via Stress-Induced Mechanical Buckling Instabilities. *Macromolecules* **2005**, *38*, 5367-5370.
17. Wang, Q.; Schlenoff, J. B., Tough Strained Fibers of a Polyelectrolyte Complex: Pretensioned Polymers. *RSC Advances* **2014**, *4*, 46675-46679.
18. Onogi, S.; Sasaguri, K.; Adachi, T.; Ogihara, S., Time–Humidity Superposition in Some Crystalline Polymers. *Journal of Polymer Science* **1962**, *58*, 1-17.
19. Nolte, A. J.; Treat, N. D.; Cohen, R. E.; Rubner, M. F., Effect of Relative Humidity on the Young's Modulus of Polyelectrolyte Multilayer Films and Related Nonionic Polymers. *Macromolecules* **2008**, *41*, 5793-5798.
20. Suarez-Martinez, P. C.; Batys, P.; Sammalkorpi, M.; Lutkenhaus, J. L., Time–Temperature and Time–Water Superposition Principles Applied to Poly(Allylamine)/Poly(Acrylic Acid) Complexes. *Macromolecules* **2019**, *52*, 3066-3074.
21. Yano, O.; Wada, Y., Effect of Sorbed Water on Dielectric and Mechanical Properties of Polyion Complex. *Journal of Applied Polymer Science* **1980**, *25*, 1723-1735.
22. Farhat, T.; Yassin, G.; Dubas, S. T.; Schlenoff, J. B., Water and Ion Pairing in Polyelectrolyte Multilayers. *Langmuir* **1999**, *15*, 6621-6623.
23. Ohno, H.; Shibayama, M.; Tsuchida, E., DSC Analyses of Bound Water in the Microdomains of Interpolymer Complexes. *Die Makromolekulare Chemie* **1983**, *184*, 1017-1024.
24. Li, H.; Lalwani, S. M.; Eneh, C. I.; Braide, T.; Batys, P.; Sammalkorpi, M.; Lutkenhaus, J. L., A Perspective on the Glass Transition and the Dynamics of Polyelectrolyte Multilayers and Complexes. *Langmuir* **2023**, *39*, 14823-14839.
25. Batys, P.; Zhang, Y.; Lutkenhaus, J. L.; Sammalkorpi, M., Hydration and Temperature Response of Water Mobility in Poly(Diallyldimethylammonium)–Poly(Sodium 4-Styrenesulfonate) Complexes. *Macromolecules* **2018**, *51*, 8268-8277.
26. Akkaoui, K.; Digby, Z. A.; Do, C.; Schlenoff, J. B., Comprehensive Dynamics in a Polyelectrolyte Complex Coacervate. *Macromolecules* **2024**, *57*, 1169-1181.
27. Schaaf, P.; Schlenoff, J. B., Saloplastics: Processing Compact Polyelectrolyte Complexes. *Advanced Materials* **2015**, *27*, 2420-2432.
28. Fares, H. M.; Wang, Q.; Yang, M.; Schlenoff, J. B., Swelling and Inflation in Polyelectrolyte Complexes. *Macromolecules* **2018**, *52*, 610-619.
29. Zhang, B.; Hoagland, D. A.; Su, Z., Ionic Liquids as Plasticizers for Polyelectrolyte Complexes. *The Journal of Physical Chemistry B* **2015**, *119*, 3603-3607.
30. Chen, Y.; Shull, K. R., Processing Polyelectrolyte Complexes with Deep Eutectic Solvents. *ACS Macro Letters* **2021**, *10*, 1243-1247.

31. Michaels, A. S.; Miekka, R. G., Polycation-Polyanion Complexes: Preparation and Properties of Poly-(Vinylbenzyltrimethylammonium) Poly-(Styrenesulfonate). *J. Phys. Chem.* **1961**, *65*, 1765-1773.
32. Leader, G. R., The Dielectric Constant of Formamide 1. *Journal of the American Chemical Society* **1951**, *73*, 856-857.
33. Perticaroli, S.; Comez, L.; Sassi, P.; Morresi, A.; Fioretto, D.; Paolantoni, M., Water-Like Behavior of Formamide: Jump Reorientation Probed by Extended Depolarized Light Scattering. *The Journal of Physical Chemistry Letters* **2018**, *9*, 120-125.
34. Kiss, B.; Fábián, B.; Idrissi, A.; Szőri, M.; Jedlovszky, P., Miscibility and Thermodynamics of Mixing of Different Models of Formamide and Water in Computer Simulation. *The Journal of Physical Chemistry B* **2017**, *121*, 7147-7155.
35. Jasien, P. G.; Stevens, W. J., Ab Initio Study of the Hydrogen Bonding Interactions of Formamide with Water and Methanol. *The Journal of Chemical Physics* **1986**, *84*, 3271-3277.
36. Fuchs, J.; Dell'Attì, D.; Buhot, A.; Calemczuk, R.; Mascini, M.; Livache, T., Effects of Formamide on the Thermal Stability of DNA Duplexes on Biochips. *Analytical Biochemistry* **2010**, *397*, 132-134.
37. Shivaglal, M. C.; Singh, S., Effect of Hydrogen Bonding and Cooperativity on Stretching Force Constants of Formamide. *International Journal of Quantum Chemistry* **1992**, *44*, 679-690.
38. Cheeseman, J. R.; Carroll, M. T.; Bader, R. F. W., The Mechanics of Hydrogen Bond Formation in Conjugated Systems. *Chemical Physics Letters* **1988**, *143*, 450-458.
39. Blake, R. D.; Delcourt, S. G., Thermodynamic Effects of Formamide on DNA Stability. *Nucleic Acids Research* **1996**, *24*, 2095-2103.
40. Kamineni, V. K.; Lvov, Y. M.; Dobbins, T. A., Layer-by-Layer Nanoassembly of Polyelectrolytes Using Formamide as the Working Medium. *Langmuir* **2007**, *23*, 7423-7427.
41. Digby, Z. A.; Yang, M.; Lteif, S.; Schlenoff, J. B., Salt Resistance as a Measure of the Strength of Polyelectrolyte Complexation. *Macromolecules* **2022**, *55*, 978-988.
42. Akintola, J.; Digby, Z. A.; Schlenoff, J. B., Polyelectrolyte Complexes as Desiccants: Thirsty Saloplastics. *ACS Applied Materials & Interfaces* **2023**, *15*, 9962-9969.
43. Chen, Y.; Yang, M.; Schlenoff, J. B., Glass Transitions in Hydrated Polyelectrolyte Complexes. *Macromolecules* **2021**, *54*, 3822-3831.
44. Drăgan, D., Water-Soluble Polymers by Interaction of Sulfonic Polyelectrolytes with Dipolar Aprotic Solvents. *Die Angewandte Makromolekulare Chemie* **1996**, *236*, 85-95.
45. Drăgan, D., Polymers with Pendent Arylsulfonamide Groups by Interaction of Sulfonic Polyacids with Amidic Solvents. *European Polymer Journal* **1998**, *34*, 1085-1092.
46. Gooda, S. R.; Huglin, M. B., New Water-Soluble Polymers and Copolymers by Interaction of Polyelectrolytes with Formamide. *Journal of Polymer Science Part A: Polymer Chemistry* **1992**, *30*, 1549-1557.
47. Cundall, R. B.; Lawton, J. B.; Murray, D.; Phillips, G. O., Polyelectrolyte Complexes, 1. The Effect of pH and Ionic Strength on the Stoichiometry of Model Polycation—Polyanion Complexes. *Die Makromolekulare Chemie* **1979**, *180*, 2913-2922.
48. Trinh, C. K.; Schnabel, W., Ionic-Strength Dependence of the Stability of Polyelectrolyte Complexes - Its Importance for the Isolation of Multiply-Charged Polymers. *Angew Makromol Chem* **1993**, *212*, 167-179.

49. Dautzenberg, H.; Kriz, J., Response of Polyelectrolyte Complexes to Subsequent Addition of Salts with Different Cations. *Langmuir* **2003**, *19*, 5204-5211.

50. Fu, J.; Fares, H. M.; Schlenoff, J. B., Ion-Pairing Strength in Polyelectrolyte Complexes. *Macromolecules* **2017**, *50*, 1066-1074.

51. Priftis, D.; Tirrell, M., Phase Behaviour and Complex Coacervation of Aqueous Polypeptide Solutions. *Soft Matter* **2012**, *8*, 9396-9405.

52. Wang, Q. F.; Schlenoff, J. B., The Polyelectrolyte Complex/Coacervate Continuum. *Macromolecules* **2014**, *47*, 3108-3116.

53. Ali, S.; Prabhu, V. M., Relaxation Behavior by Time-Salt and Time-Temperature Superpositions of Polyelectrolyte Complexes from Coacervate to Precipitate. *Gels* **2018**, *4*.

54. Meng, S.; Ting, J. M.; Wu, H.; Tirrell, M. V., Solid-to-Liquid Phase Transition in Polyelectrolyte Complexes. *Macromolecules* **2020**, *53*, 7944-7953.

55. Safronov, A. P.; Kamalov, I. A., The Parameter of Binary Interaction in Weakly Crosslinked Polyelectrolyte Gels near the Collapse Threshold. *Polym Sci Ser A* **2011**, *53*, 195-203.

56. Duignan, T. T.; Zhao, X. S., The Born Model Can Accurately Describe Electrostatic Ion Solvation. *Physical Chemistry Chemical Physics* **2020**, *22*, 25126-25135.

57. Salehi, A.; Larson, R. G., A Molecular Thermodynamic Model of Complexation in Mixtures of Oppositely Charged Polyelectrolytes with Explicit Account of Charge Association/Dissociation. *Macromolecules* **2016**, *49*, 9706-9719.

58. Yang, M.; Sonawane, S. L.; Digby, Z. A.; Park, J. G.; Schlenoff, J. B., Influence of "Hydrophobicity" on the Composition and Dynamics of Polyelectrolyte Complex Coacervates. *Macromolecules* **2022**, *55*, 7594-7604.

59. Fu, J. C.; Schlenoff, J. B., Driving Forces for Oppositely Charged Polyion Association in Aqueous Solutions: Enthalpic, Entropic, but Not Electrostatic. *Journal of the American Chemical Society* **2016**, *138*, 980-990.

60. Yang, M.; Digby, Z. A.; Schlenoff, J. B., Precision Doping of Polyelectrolyte Complexes: Insight on the Role of Ions. *Macromolecules* **2020**, *53*, 5465-5474.

61. Fu, J. C.; Abbott, R. L.; Fares, H. M.; Schlenoff, J. B., Water and the Glass Transition Temperature in a Polyelectrolyte Complex. *Acs Macro Letters* **2017**, *6*, 1114-1118.

62. Rubinstein, M.; Colby, R. H., *Polymer Physics*. Oxford University Press: New York, 2003.

63. Larson, R. G.; Liu, Y.; Li, H., Linear Viscoelasticity and Time-Temperature-Salt and Other Superpositions in Polyelectrolyte Coacervates. *Journal of Rheology* **2021**, *65*, 77-102.

64. Perry, S. L.; Leon, L.; Hoffmann, K. Q.; Kade, M. J.; Priftis, D.; Black, K. A.; Wong, D.; Klein, R. A.; Pierce, C. F., 3rd; Margossian, K. O.; Whitmer, J. K.; Qin, J.; de Pablo, J. J.; Tirrell, M., Chirality-Selected Phase Behaviour in Ionic Polypeptide Complexes. *Nat. Commun.* **2015**, *6*, 6052.

65. Boulmedais, F.; Schwinté, P.; Gergely, C.; Voegel, J. C.; Schaaf, P., Secondary Structure of Polypeptide Multilayer Films: An Example of Locally Ordered Polyelectrolyte Multilayers. *Langmuir* **2002**, *18*, 4523-4525.

66. Bosshard, H. R.; Marti, D. N.; Jelesarov, I., Protein Stabilization by Salt Bridges: Concepts, Experimental Approaches and Clarification of Some Misunderstandings. *J. Mol. Recognit.* **2004**, *17*, 1-16.

67. Hendsch, Z. S.; Tidor, B., Do Salt Bridges Stabilize Proteins? A Continuum Electrostatic Analysis. *Protein Sci* **1994**, *3*, 211-226.

68. Anslyn, E. V.; Dougherty, D. A., *Modern Physical Organic Chemistry*. University Science Books: Sausalito, CA, 2006.

69. Shaheen, S. A.; Yang, M.; Chen, B.; Schlenoff, J. B., Water and Ion Transport through the Glass Transition in Polyelectrolyte Complexes. *Chemistry of Materials* **2020**, *32*, 5994-6002.

70. Yang, M.; Epps, T. H., III, Solid-State, Single-Ion Conducting, Polymer Blend Electrolytes with Enhanced  $\text{Li}^+$  Conduction, Electrochemical Stability, and Limiting Current Density. *Chemistry of Materials* **2024**, *36*, 1855-1869.

71. Wang, Y.; Fan, F.; Agapov, A. L.; Yu, X.; Hong, K.; Mays, J.; Sokolov, A. P., Design of Superionic Polymers—New Insights from Walden Plot Analysis. *Solid State Ionics* **2014**, *262*, 782-784.

72. Pazmiño Betancourt, B. A.; Hanakata, P. Z.; Starr, F. W.; Douglas, J. F., Quantitative Relations between Cooperative Motion, Emergent Elasticity, and Free Volume in Model Glass-Forming Polymer Materials. *Proceedings of the National Academy of Sciences* **2015**, *112*, 2966-2971.

73. Lide, D. R.; Milne, G. W., *Handbook of Data on Common Organic Compounds*. CRC press: Boca Raton, 1995; Vol. Vol. 3.

### Table of Contents Graphic

